NASA

FINAL REPORT

EXPERIMENTAL SCALING STUDY OF FLUID AMPLIFIER ELEMENTS

By

ISAAC GREBER

CHARLES TAFT

JOSEPH ABLER

Prepared For

GEORGE C. MARSHALL SPACE FLIGHT CENTER

NATIONAL AERONAUTICS AND SPACE ADMINISTRATION

HUNTSVILLE, ALABAMA

MARCH 31, 1966

GPO PRICE $ _____

CFSTI PRICE(S) $ _____

CONTRACT NAS8-11267

Hard copy (HC) 2.00

Microfiche (MF) .50

ff 653 July 65

CASE INSTITUTE OF TECHNOLOGY

CLEVELAND, OHIO

ABSTRACT

Scaling parameters of three fluid amplifier elements are investigated experimentally. The elements are a bistable device, a boundary layer control device , and a vortex device. Appropriate parameters for presentation of the experimental data are determined by dimensional analysis. The large number of non-dimensional parameters in considerably reduced by physical reasoning, to produce relatively simple correlation schemes. Despite the major geometrical differences among the elements, the simplified correlation schemes are remarkably similar.

Experimental data is presented grouped according to the simplified correlation schemes. The experiments show that there exist ranges of operation in which performance varies only weakly with Reynolds number, and that there exist ranges in which the performance parameters appear only in combination, which results in important additional simplification of the experimental correlations. Ranges in which the simplified correlations are expected to break down, and use of the scaling ideas for other elements, are discussed.

Author

Table of Contents

List of Figures

List of Symbols

a	speed of sound
D	diameter
d_o	outlet diameter of vortex element
d_1	major diameter of vortex element
d_s	annular width of supply chamber of vortex element
h	spacing between walls of vortex element (corresponds to L_2)
L	length
L_1	characteristic length in planform (usually nozzle width)
L_2	characteristic length perpendicular to planform
M	Mach number = $\frac{\text{flow speed}}{\text{sound speed}}$
P	$p - p_v$
p	pressure
Q	volume flow rate
Re	Reynolds number
r	radius
V	velocity
w	control port width of vortex element (corresponds to L_1) See Fig. 11
ϵ	size of roughness element
μ	dynamic viscosity coefficient
ν	kinematic viscosity coefficient = μ/ρ
ρ	density = mass per unit volume
ω	angular frequency

Pressure and Volume Flow Rate Subscripts

1	wall attachment side
2	side opposite wall attachment side
c	control
o	outlet
s	supply
t	total (or stagnation)
v	vent

INTRODUCTION

This study examines some of the scaling parameters of three fluid amplifier elements. The elements are a bistable device, a boundary layer control device, and a vortex device. The basic idea in all these devices, as in all fluid amplifiers, is as follows: A supply of fluid enters a box which has one or more outlet holes, one or more control flow holes, and one or more auxiliary holes. For some fixed supply condition, for example, a fixed reservoir pressure from which the supply flow comes, the relatively large amount of fluid which leaves through an outlet hole is determined by a relatively small amount of fluid entering through a control flow hole.

This study is concerned primarily with the manner in which the performance scales; that is, how the performance varies with size, fluid, and other conditions. It is not concerned with element design. For the purpose of determining the scaling laws we examine experimentally the non-dimensional performance of geometrically similar elements, choosing designs which have previously been developed. We restrict our consideration to single fluid operation (that is the surrounding atmosphere consists of the same kind offluid as the supply fluid), and report on experiments in air and in water. For the most part we consider sufficiently low fluid speeds so that air can be regarded as incompressible. As is common in fluid amplifier work, we restrict consideration to geometries in which the intended operation is two-dimensional; consequently similarity means maintaining similar planforms. Since physical elements do not behave two-dimensionally, we examine to some extent effects of varying the length perpendicular to the representative plane of the planform. We consider only steady flow.

Even with the restrictions imposed, the number of variables remains too large for convenient use. Consequently a major object of this study is the determination of ranges of operation in which some of the variables are not very important, and the establishment of ways of compacting the data. Hopefully these simplifications can be applied to other elements. Obviously, an important by-product of the attempt to establish scaling laws is the actual performance characteristics of the particular elements investigated.

In discussing the scaling laws for the different elements, we proceed by first performing a straightforward dimensional analysis, then discuss reduction of the number of non-dimensional parameters through various physical assumptions, then examine how the experimental data correlates according to the simplified schemes, then consider when the simplified correlation might break down. It will be clear that not only the approach but also some of the simplified correlation schemes will be applicable to other elements. To keep the physical assumptions clear, they will be made within the framework of the geometry of the particular elements, but their extension to more general elements should be kept in mind, and will occasionally be pointed out.

Bistable Element

(1) General Description

This is an element in which a supply jet attaches to one of two nearby walls. The detailed geometry is shown in Figure 1. The letters in the figure refer to supply, control, vent, and outlet, in a rather self-defining notation. The jet remains attached to wall No. 1 until the control flow rate reaches some critical value. Then it switches to wall No. 2. The type of element is well known. The particular geometry we investigate is the one developed by J. N. Wilson (Ref 1).

We characterize the supply and control pressures by settling chamber values (i.e. we use stagnation pressures p_{s_t} and p_{c_t} where the subscript t means total , another word signifying stagnation conditions). We characterize the outlet pressure by the static pressure at the outlet leg, and the vent pressure by the pressure of the surrounding atmosphere. Choosing stagnation values of supply and control pressure means that we regard the entrance nozzles as basically part of the design of the element. Choosing static pressures at outlet and vent means that we do not want to prejudge the nature of a connection at the exit. If we imagine jets exiting into a reservoir, then the reservoir pressure will impose itself as the static pressure of the exiting jet. Of course, if flow enters through the vent, then the atmospheric pressure is the stagnation pressure for the entering vent fluid. We characterize the flow through each hole by a volume flow rate Q, which is a measure of the average velocity. We characterize the planform by a length L_1 (in all calculations we take this length to be the width of the supply nozzle at its exit, and hence the width of the supply jet), and the length perpendicular to the platform by L_2. Because the planform remains fixed in the study of a perticular element, these two lengths are sufficient to describe the geometry.

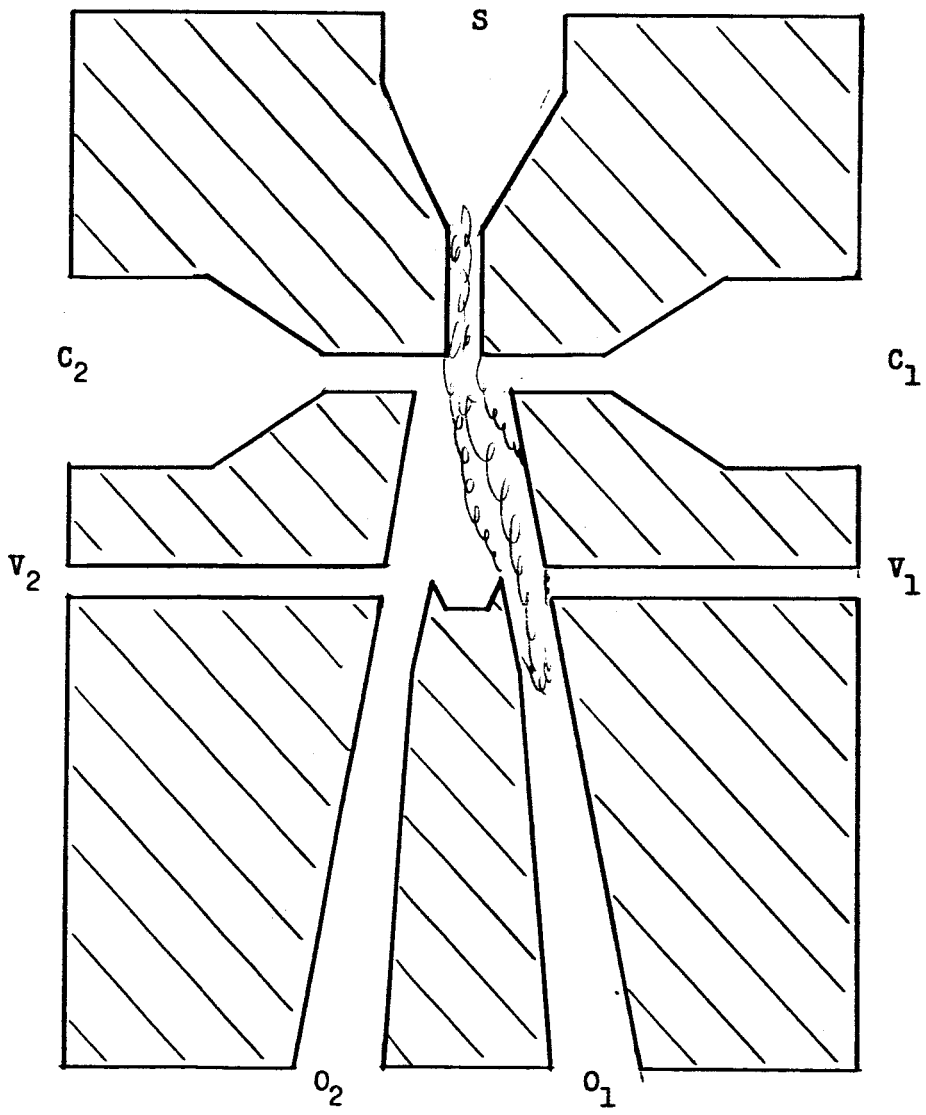

FIGURE 1 BISTABLE ELEMENT

(2) Performance Parameters

The basic variables are:

$$p_{s_t},\ p_{c_{1_t}},\ p_{c_{2_t}},\ p_{v_1},\ p_{o_1},\ p_{o_2},\ Q_s,\ Q_{c_1},\ Q_{c_2},\ Q_{v_1},\ Q_{v_2},\ Q_{o_1},\ Q_{o_2},\ \rho,\ \mu,\ a,\ L_1,\ L_2$$

Since we immerse the element in a single atmosphere, $p_{v_1} = p_{v_2} \equiv p_v$. It seems reasonable that pressure difference should be significant rather than pressure levels (except as the pressure level affects the density), and hence we use the difference between pressure and vent pressure as the pertinent variable. We can eliminate one of the flow rates by conservation of mass. Since we really are not interested in the vent flow, we regard $Q_{v_1} + Q_{v_2}$ as a single variable and eliminateit by conservation of mass. The reduced set of variables is:

$$(p_{s_t} - p_v),\ (p_{c_{1_t}} - p_v),\ (p_{c_{2_t}} - p_v),\ (p_{o_1} - p_v),\ (p_{o_2} - p_v),\ Q_s,\ Q_{c_1},\ Q_{c_2},\ Q_{o_1},\ Q_{o_2},\ \rho,\ \mu,\ a,\ L_1,\ L_2 \qquad (1)$$

This is a set of 15 variables. Using mass, length, time as fundamental dimensions we can form 12 independent non-dimensional parameters. One set is:

$$\frac{p_{o_1} - p_v}{p_{s_t} - p_v},\ \frac{p_{o_2} - p_v}{p_{s_t} - p_v},\ \frac{p_{c_{1_t}} - p_v}{p_{s_t} - p_v},\ \frac{p_{c_{2_t}} - p_v}{p_{s_t} - p_v},\ \frac{Q_{c_1}}{Q_s},\ \frac{Q_{c_2}}{Q_s},\ \frac{Q_{o_1}}{Q_s},\ \frac{Q_{o_2}}{Q_s},$$

$$\frac{L_2}{L_1},\ \left(\frac{2\rho Q_s}{\mu(L_2 + L_1)}\right),\ \frac{(p_{s_t} - p_v)\, L_1^2}{p(Q_2/L_2)^2},\ \frac{Q_s}{L_1 L_2 a} \qquad (2)$$

Only the last three parameters need any discussion. First consider the Reynolds number $Re \equiv \frac{2\rho Q_s}{\mu (L_1 + L_2)}$

This is a Reynolds based on average velocity and hydraulic diameter; that is

$$Re = \frac{\rho V_{avg} D_{hyd}}{\mu} = \left(\frac{\rho Q_s}{\mu L_1 L_2}\right) \frac{4 L_1 L_2}{2(L_1 + L_2)} = \frac{2\rho Q_s}{\mu(L_1 + L_2)}$$

Note that alternative independent pairs Re and L_2/L_1 could be formed from the ones used in these calculations.

The eleventh parameter is the pressure coefficient $c_{p_{s_t}} \equiv \frac{(p_{s_t} - p_v) L_1^2}{\rho (Q_s/L_2)^2}$

The important thing to note here is the existance of the pressure coefficient as a parameter, not its arbitrary form. If convenient, we can replace this form by another, for example using the pressure difference between supply and outlet. This point of view is useful to our later discussions.

Completing our dozen is the Mach number, $\frac{Q_s}{L_1 L_2 a}$, the ratio of flow speed to sound speed "a." Our experiments are in a range of M<0.3, so that we will not have to consider this as a variable, (but we have to keep it in mind). Correspondingly we can consider the density to be constant.

It is important to examine whether the number of parameters can be reduced. Reduction can occur because of weak variation with a parameter, because parameters appear only in combination, or because a sub-group is physically related. As an example of the last idea, recall that we eliminated one volume flow rate through mass conservation. It is also important to examine whether an important variable has been left out. In general this will be made evident by the failure of preformance to correlate according to the

assumed variables.

(3) Reduction of Parameters

The most sweeping reduction is obtained by recognizing that there is a range of operation, and it is probably the practical range, in which the side of the element opposite to the attached flow (the inactive side, denoted by subscripts 2 before) is essentially characterized by negligible flow and by vent pressure. This eliminates the four parameters involving p_{o_2}, p_{c_2}, Q_{o_2}, α_{c_2}.

At this stage it is convenient to think of our set of remaining parameters as forming the following functional equation:

$$\frac{Q_{o_1}}{Q_s} = \frac{p_{o_1} - p_v}{p_{s_t} - p_v}, \frac{p_{c_{1_t}} - p_v}{p_{s_t} - p_v}, \frac{Q_{c_1}}{Q_s}, \frac{2\rho Q_s}{\mu(L_2 + 1)} \frac{(p_{s_t} - p_v)L_1^2 L_2^2}{\rho Q_s^2}, \frac{L_2}{L_1} \qquad (3)$$

We can anticipate elimination of one parameter, the pressure coefficient, by imagining that some interior pressure exists, which determines flow rates through the several holes. This is somewhat equivalent to regarding the several holes as independent orifices. The value of the interior pressure, and hence the flow rates, are determined by the requirement that the same pressure result from the s several flow rates through the different orifices; this matching condition serves to eliminate one parameter. Note that this is a physical oversimplification, which may sometimes be invalid. The final reduction stems from the experimental observation that the control flow only weakly affects the ratio of output to supply flow. The reason is that relatively small control flow rates are required for the full range of operation, up to switching; naturally, one designs an element such that only small control flow is required. The reduced functional equation is:

$$\frac{Q_{o_1}}{Q_s} = f\left(\frac{p_{o_1} - p_v}{p_{s_t} - p_v}, \frac{2\rho Q_s}{\mu(L_2 + L_1)}, \frac{L_2}{L_1}\right) \qquad (4)$$

Instead of eliminating the pressure coefficient, we could have solved for it. The above argument says that we could have eliminated Q_{o_1} / Q_s. Thus one gets

$$\frac{\left(p_{s_t} - p_v\right) L_1^2 L_2^2}{\rho Q_s^2} = f\left(\frac{p_{o_1} - p_v}{p_{s_t} - p_v}, \frac{2\rho Q_s}{\mu(L_2 + L_1)}, \frac{L_2}{L_1}\right) \qquad (4a)$$

We plot in the form (4) rather than (4a), but it is useful to keep in mind the corresponding existance of the correlation (4a).

(4) Experimental Procedure

Measurements were made on three elements, whose planform is shown in Figure 1. In all elements the nozzle width L_1 was 1/32". Measurements in air were made with transverse lengths L_2 of 0.025", 0.050", 0.102". (Note that Wilson's measurements (Ref. 1) were made on an element with L_1=1/32" and L_2 = 0.050"). Measurements in water were made with the element having L_2 = 0.50". The test set-up is shown in Figure 2.

Pressure taps were located in large area sections just upstream of the supply and control ports and just downstream of the outlet ports. Pressure differences from room pressure were measured in either mercury or water manometers. Flow rates were measured on Fisher-Porter rotameters, whose factory calibration was spot checked.

When measuring in water, the trough was filled with water to the top of the element, which was sufficient to well submerge the vents. Because of the small height of water above the vent, vent pressure was still taken to be the room pressure.

Temperatures were recorded of the air or water before it entered the element. Time was allowed for temperatures to reach a steady state value before taking performance data. Temperature measurement is particularly important with water because of the large variation of viscosity with temperature.

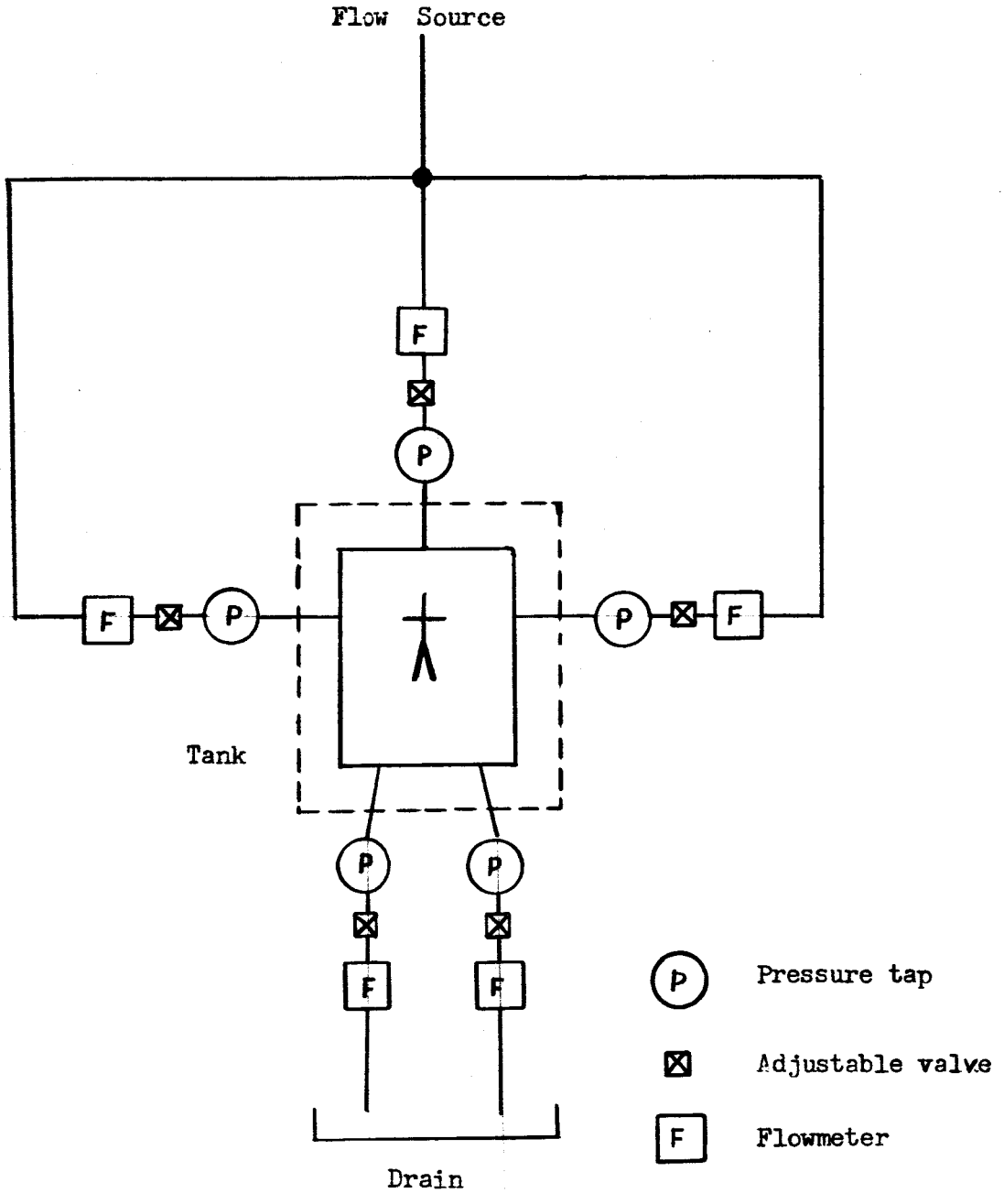

FIGURE 2 TEST SETUP SCHEMATIC

(5) Experimental Results

(a) Flow rate-pressure ratio curves

The flow rate-pressure ratio curves for the bistable element are shown in Figure 3, for an aspect ratio L_2/L_1, of 1.6, (that is, for the element with L_2 = 0.050). The lower two curves are shown for fixed Reynolds number. The uppermost curve is for the Reynolds number range 6,000 to 20,000; in this range, and presumably higher, the flow rate-pressure ratio relationship appears to be almost independent of Reynolds number. This indicates either that the Reynolds number dependence merely becomes weak with increasing Reynolds number, or it may even indicate an asymototic limit for infinite Reynolds number. From the point of view of designing elements, the distinction between the reasons for weak dependence on Reynolds number is not particularly important.

One notes that zero output flow is reached before the output pressure becomes equal to the supply stagnation pressure. Remember that at zero output flow, all supply flow leaves through the vents. From the point of view of our earlier discussion, zero output flow is reached when the interior pressure equals the output pressure.

On notes also that, at least at high Reynolds number, the output flow becomes larger than the supply flow, as the output pressure is reduced to the level of the vent pressure.

Some of the effects of the aspect ratio on the flow rate-pressure ratio relations are shown in Figure 4, which gives the high Reynolds number limit results for the three aspect ratios tested. Note that for the aspect ratios of 0.8 and 3.15 measurements were only made in air.

It is seen that the maximum output pressure (that is, the value obtained with no output flow) increases with increasing aspect ratio. The maximum output flow rate (that is, the value obtained with output pressure equal to the vent pressure) appears to have a peak at an intermediate aspect ratio. At present the reasons for this are not fully understood.

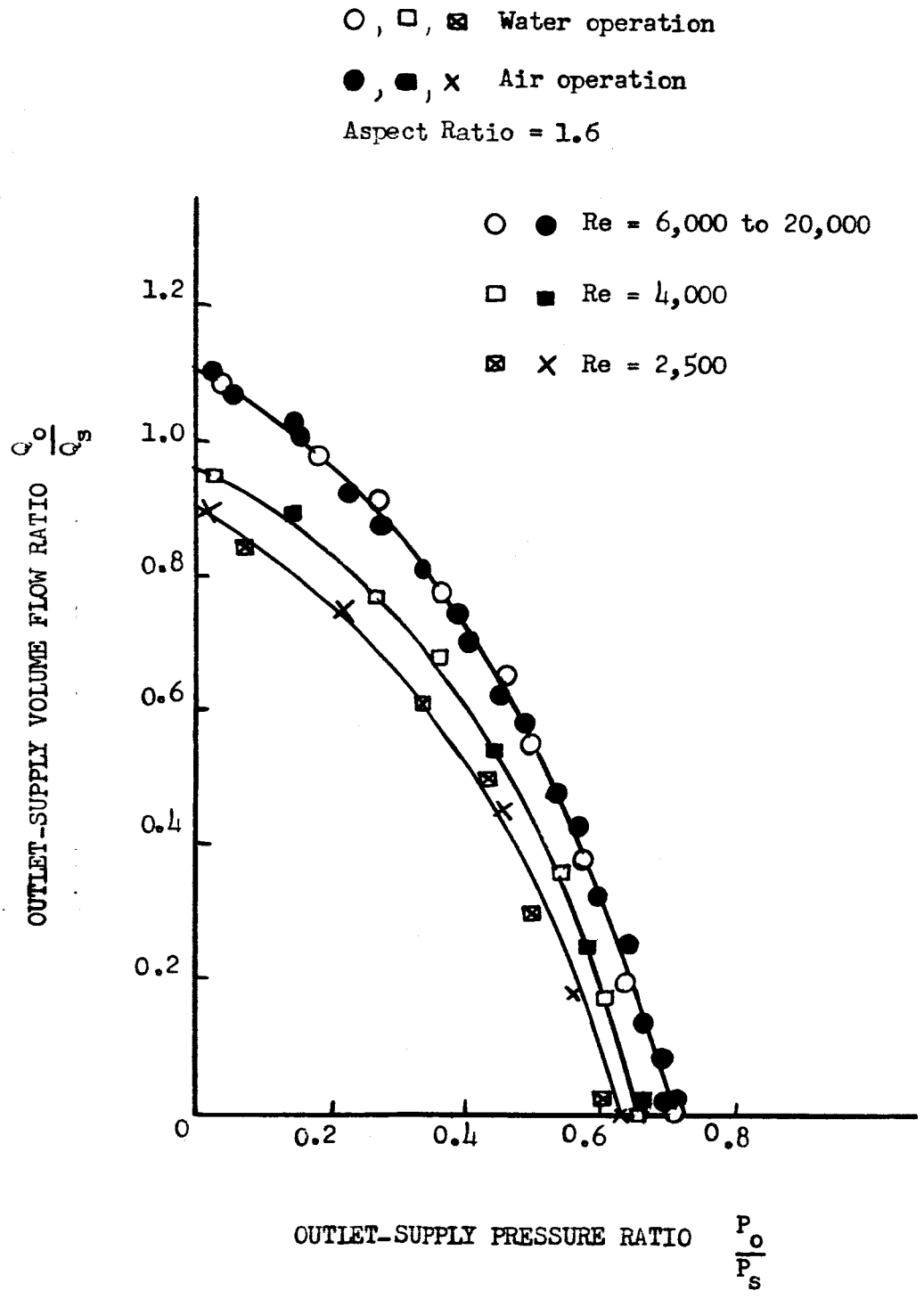

FIGURE 3 FLOW RATE-PRESSURE RATIO CURVES

Air Operation

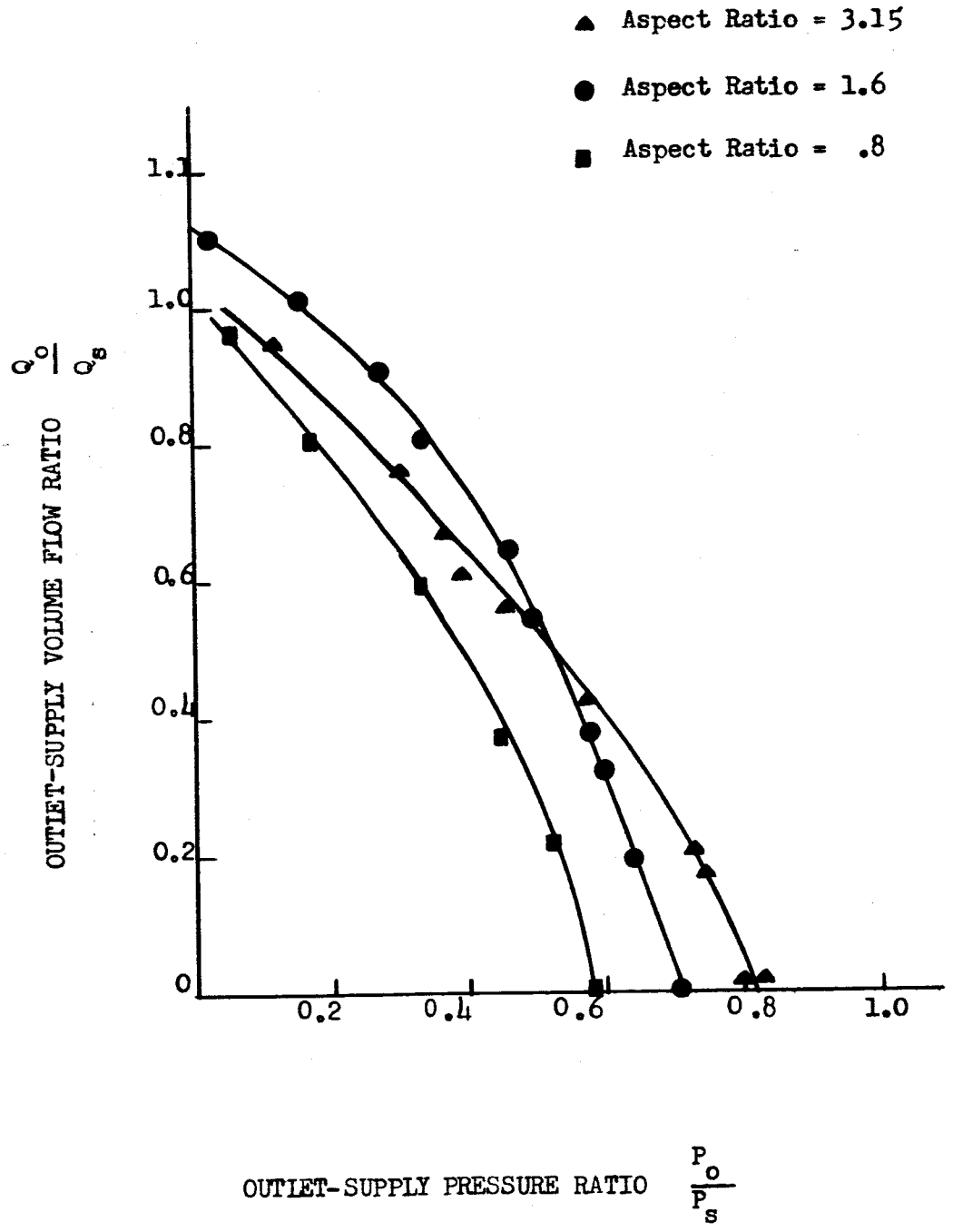

Figure 4 ASPECT RATIO EFFECTS

(b) Switching curves

Switching occurs when the attachment point reaches the end of the wall. For a given planform we can obtain a reduced set of parameters determining the attachment point by repeating the arguments leading to equation (4). We thus write:

$$x_{attachment} = f\left(\frac{p_{o_1} - p_v}{p_{s_t} - p_o}, Re, \frac{L_2}{L_1}, \frac{Q_{c_1}}{Q_s}\right) \qquad (5)$$

Here the dependence on $\frac{Q_{c_1}}{Q_s}$ is strong. Switching occurs when $\frac{x_{attachment}}{L_1}$ reaches some critical value $\frac{X_c}{L_1}$. Consequently

$$\left(\frac{Q_{c_1}}{Q_s}\right)_{switch} = f\left(\frac{p_{o_1} - p_v}{p_{s_t} - p_v}, Re, \frac{L_2}{L_1}\right) \qquad (6)$$

The switching curves are shown in Figure 5.
These curves are for Reynolds numbers of 6000 to 20,000; as with the flow rate pressure ratio curves, in this high Reynolds number range the switching characteristics are only weakly dependent on Reynolds number.

A measure of not having a fully vented inactive side is given by the curves for blocked inactive control port. It is seen that control flow rate to switch is greatly increased by blocking the opposite control port. This is physically plausible when one recognizes that blocking the opposite port is equivalent to allowing a pressure increase on the convex side of the attaching jet. From the point of view of scaling, the important thing to realize is that switching data should thus be correlated in a form equivalent to

$$\left(\frac{Q_{c_1}}{Q_s}\right)_{switch} = f\left(\frac{p_{o_1} - p_v}{p_{s_t} - p_v}, Re, \frac{L_2}{L_1}, \frac{Q_{c_2}}{Q_s}\right) \qquad (7)$$

Note that the apparent control flow rate required for switching with blocked opposite port is about 10% to 15% lower for water than for air operation. The

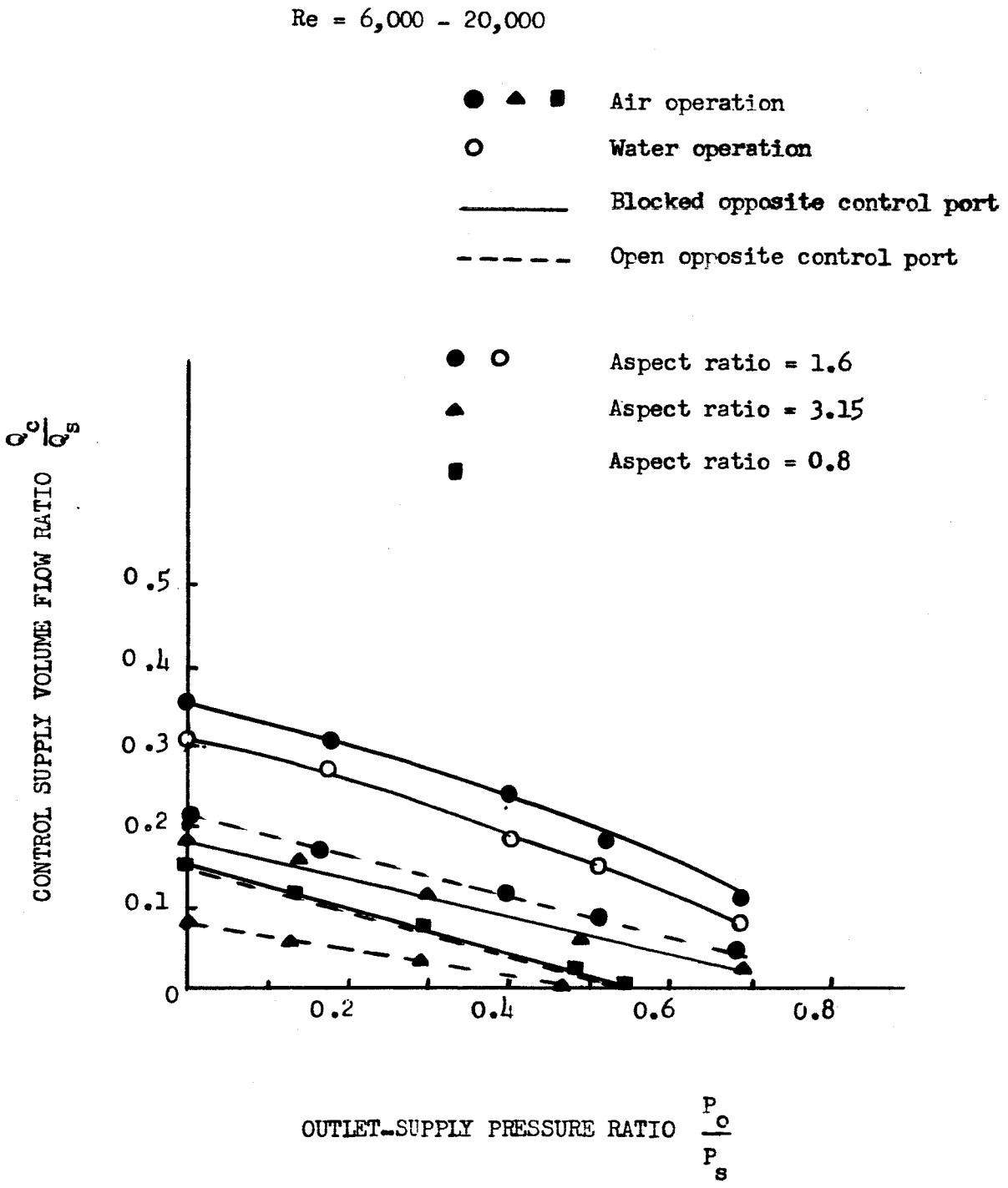

FIGURE 5 CONTROL FLOW RATE FOR SWITCHING

Re ≈ 6,000 to 20,000

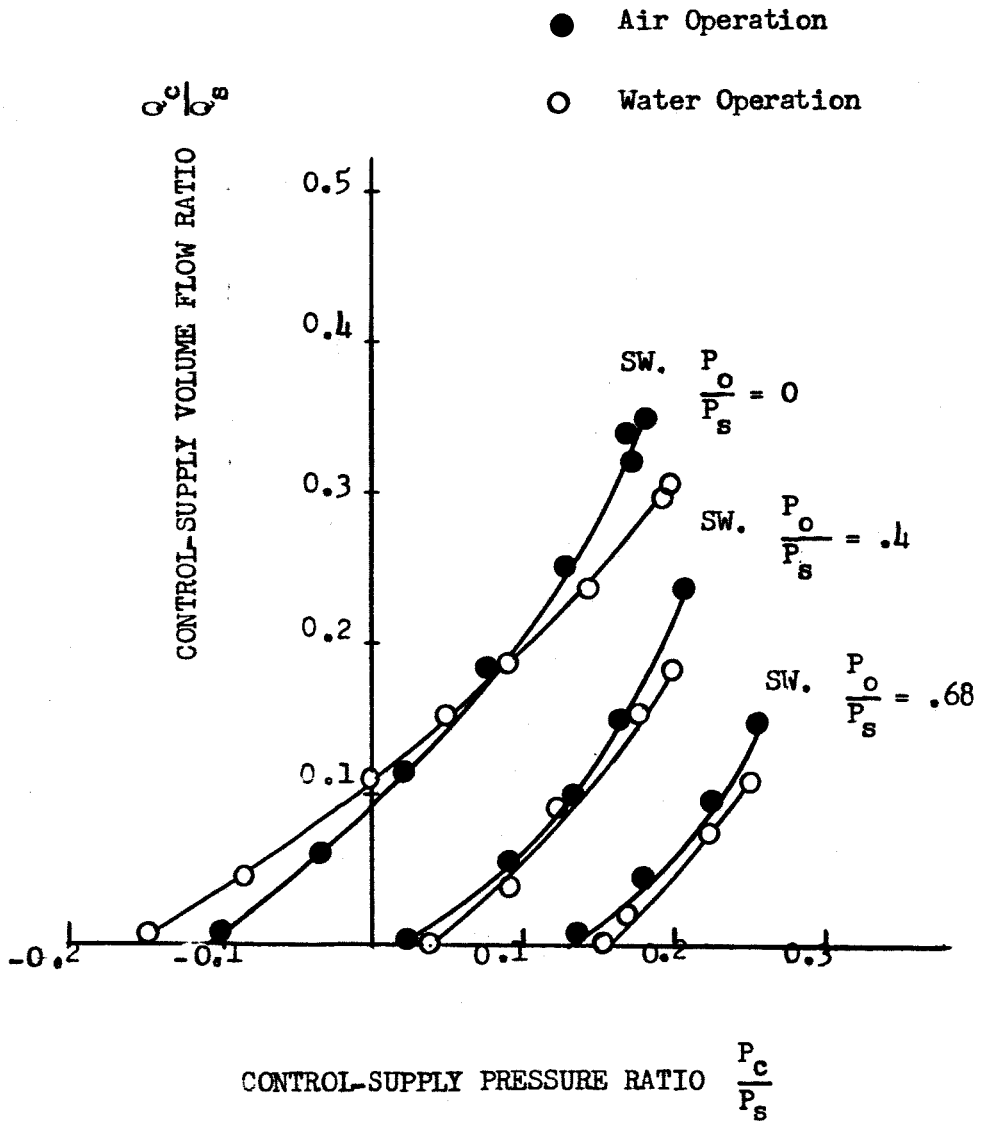

FIGURE 6 TYPICAL CONTROL FLOW-CONTROL PRESSURE RELATIONS

reasons for this are not clear. The differences, however, are sufficiently small so that we do not at this stage search for another scaling parameter, but rather suggest the continued use of eqs. (6) or (7).

For completeness, note that the switching points were determined as the end points of curves of

$$Q_{c_1/Q_s} \quad \text{vs} \quad \frac{p_{c_{t_1}} - p_v}{p_{s_t} - p_v} \quad ;$$

these curves are shown in Figure (6).

There is an interesting effect of aspect ratio shown in Figure 5. One sees that there is an apparent peak in the control flow rate required for switching at an intermediate aspect ratio. Qualitatively this looks as follows, for both open and blocked opposite control port:

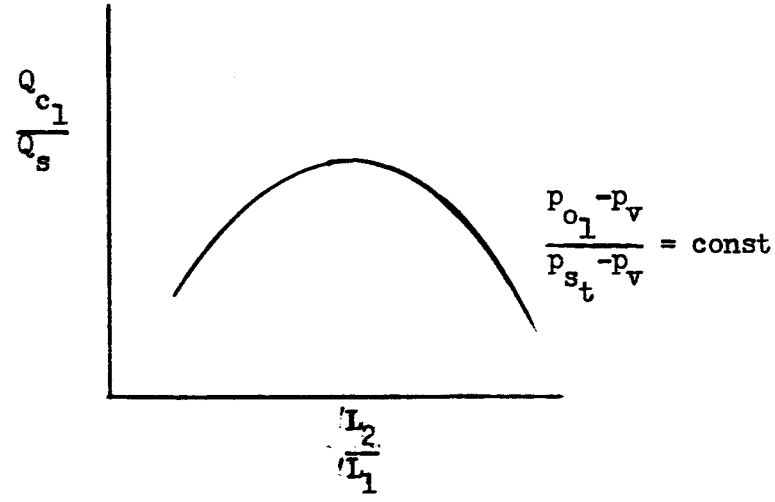

(6) Anticipated breakdown of simple correlations

The simple correlations are the result of restriction of ranges of parameter variation. They may break down when the ranges are exceeded. Thus one anticipates breakdown of the simple correlations at sufficiently low Reynolds number, and at Mach numbers near unity. Unfortunately, if one wishes to make small elements with a gaseous fluid, one is forced to operate at either low Reynolds number or high Mach number.

Boundary Layer Control Proportional Element

(1) General Description

This is an element in which a supply jet attaches to a curved wall, in the absence of control flow. With control flow present, the jet separation point moves upstream, and so a portion of the supply flow leaves through the outlet (labeled O above). The detailed geometry is shown in Figure 7. The particular geometry we investigate is the one developed by P. A. Orner (Ref. 2). We characterize the performance by identically the same variables as for the bistable device.

(2) Performance Parameters

The basic variables are:

$$p_{s_t},\ p_{c_t},\ p_v,\ p_o,\ Q_s,\ Q_c,\ Q_o,\ Q_v,\ \rho,\ \mu,\ a,\ L_1,\ L_2$$

As in our discussion of the bistable element, we again eliminate one flow rate through conservation of mass, and measure pressure differences from vent pressure. Hence our reduced set of variables is:

$$(p_{s_t}-p_v),(p_{c_t}-p_v),(p_o-p_v),\ Q_s,\ Q_c,\ Q_1,\ \rho,\ \mu,\ a,\ L_1,\ L_2$$

This is a set of 11 variables. Again using mass, length, time as fundamental dimensions we can form 8 independent non-dimensional parameters. One set is:

$$\frac{p_o-p_v}{p_{s_t}-p_v},\ \frac{p_{c_1}-p_v}{p_{s_t}-p_v},\ \frac{Q_c}{Q_s},\ \frac{Q_o}{Q_s},\ \frac{L_2}{L_1},\ \frac{\rho Q_2^{\,2}}{\mu(L_2+L_1)},\ \frac{(p_{s_t}-p_v)L_1^{\,2}}{\rho\left(Q_s/L_2\right)^2},\ \frac{Q_2}{L_1L_2a} \tag{8}$$

All of the parameters in equation (8) have previously been discussed. We can also immediately write a reduced set of parameters, repeating virtually verbatim the bistable element discussion; here, however, the dependence on control flow rate cannot be neglected. Consequently our reduced functional equation, analogous to equation (4) is:

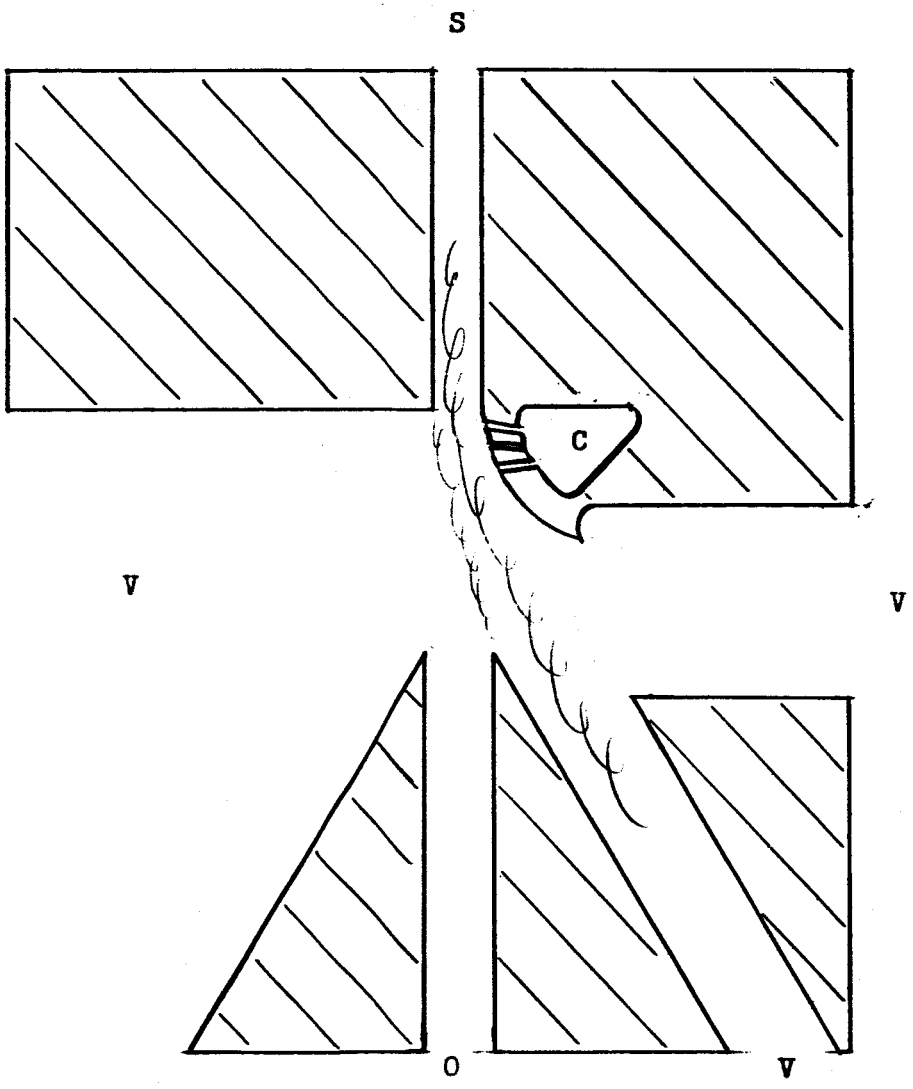

FIGURE 7 BOUNDARY LAYER CONTROL PROPORTIONAL ELEMENT

$$\frac{Q_o}{Q_s} = f\left(\frac{p_o - p_v}{p_{s_t} - p_v}, Re, \frac{Q_c}{Q_s}, \frac{L_2}{L_1}\right) \qquad (9)$$

(3) Experimental Procedure

Detailed measurements were made on one element, with nozzle width $L_1 = 1/4''$ and transverse length $L_2 = 1/4''$ (i.e., $\frac{L_2}{L_1} = 1$). In addition, some measurements were made on two smaller elements having in principle identical planforms to the larger element; one had $L_1 = L_2 = 1/16"$, the other $L_1 = 1/16"$, $L_2 = 1/8"$. The element planform is shown in Fig. 7. The smaller elements were difficult to machine accurately, and therefore are not truly geometrically similar in planform to the larger element. They were used primarily for qualitative results.

The experimental procedure was essentially the same as for the bistable element, previously discussed.

(4) Experimental Results

(a) Flow rate-pressure ratio curves

These curves are shown in Figure 8 for an aspect ratio of 1, a Reynolds number of 77,500, and a control flow ratio range of 0 to 0.34. In contradistinction with the bistable element, the output flow ratio of the proportional element is strongly dependent on control flow, and also importantly dependent on Reynolds number. The strong dependence on control flow is, of course, fundamental to the useful application of the element. As for the Reynolds number dependence, without control flow there is an asymptotic attachment angle which is only weakly dependent on control flow. However, the deviation from the asymptotic angle, and hence the amount of output flow for a given control flow ratio, is importantly dependent on Reynolds number. The asymptotic angle is reached at Re = 11,000, with no control flow.

The effect of varying Reynolds number is shown in Figure 9. The figure shows effects of Reynolds number variation for two control flow ratios, a "small" and a "large" one (.007 , .015). The strong effect of Reynolds number is clear.

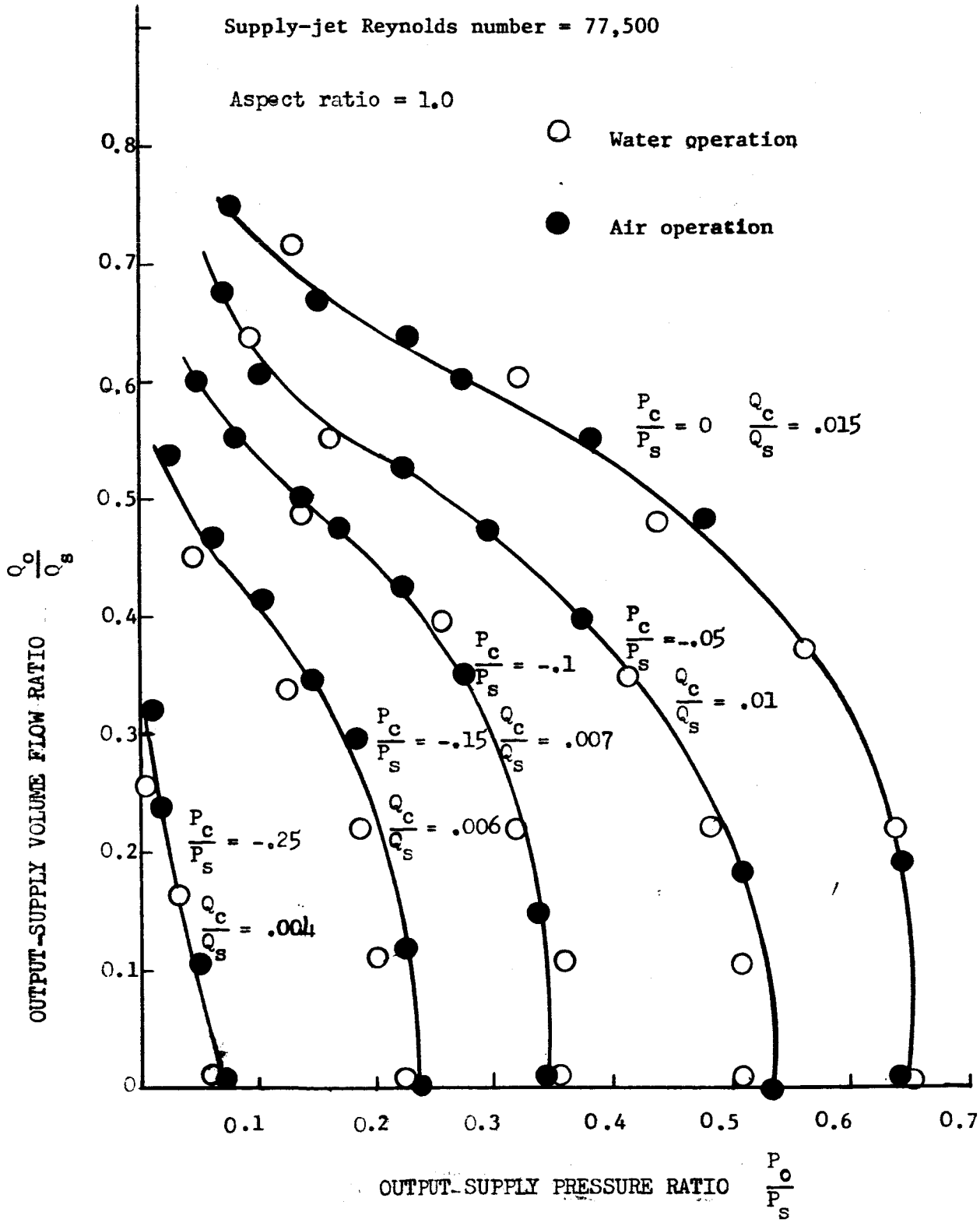

FIGURE 8 - FLOW RATE-PRESSURE RATIO CURVES

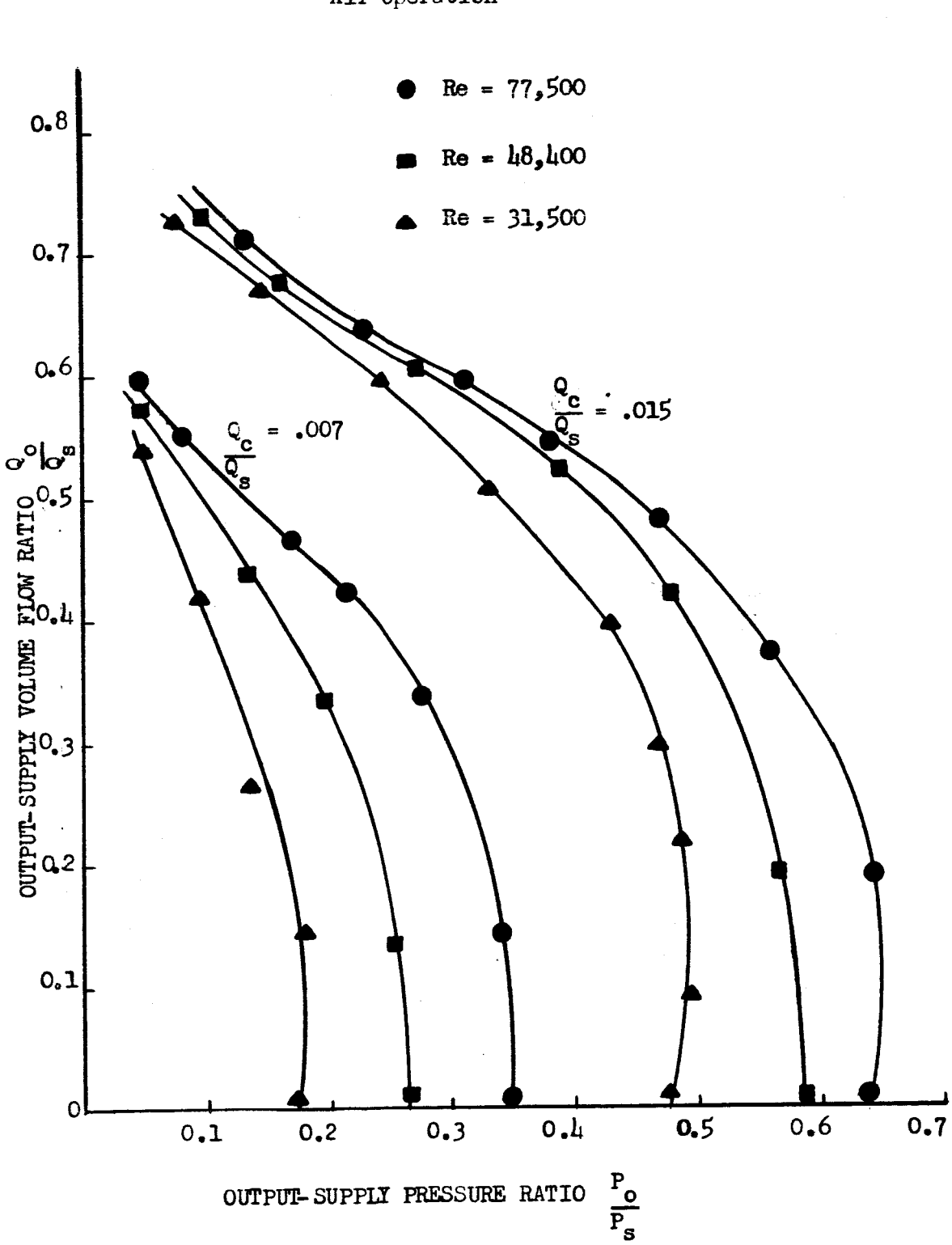

FIGURE 9 EFFECT OF REYNOLDS NUMBER ON FLOW-PRESSURE RELATIONS

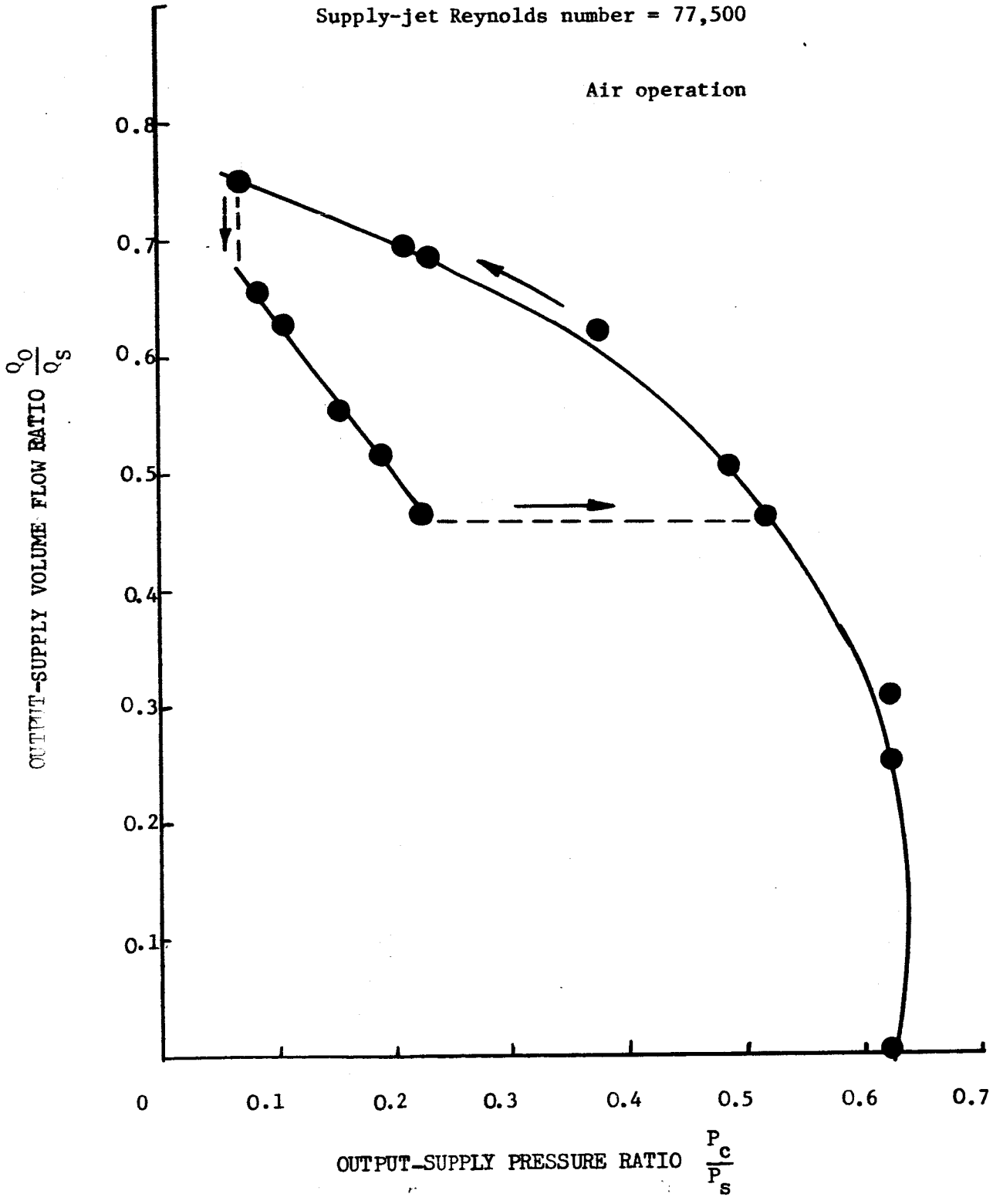

FIGURE 10 TYPICAL FLOW-PRESSURE CURVES WITH HYSTERESIS

(b) Aspect ratio effects

For this element, aspect ratio is an independent parameter. The reason for this is that the separation angle depends on Reynolds number and aspect ratio. The receiver is located so as to capture the separated jet at its high Reynolds number limit. Since this limiting angle varies with aspect ratio, a change in aspect ratio requires a change in planform. Consequently geometrically similar scaling requires maintaining constant aspect ratio.

(c) Hysteresis

If the receiver pressure is decreased, the receiver flow rate increases (all other parameters held fixed). If the receiver pressure is then increased, the flow rate decreases. As long as the receiver pressure ratio does not drop below some critical value, the same flow rate-pressure ratio curve is traced out for both increasing and decreasing receiver pressure. However, if the receiver pressure is allowed to drop below some critical value, then the same curve is not retraced on increasing pressure; instead, one observes a hysteresis loop. Figure 10 shows a typical hysteresis curve, taken with atmospheric pressure in the control flow chamber. At this condition the supply jet is essentially un-attached, and there is maximum flow rate ratio into the receiver. For smaller control flow rates, the hysteresis loop is smaller.

(d) Wall roughness

No quantitative measurements were made to evaluate the effect of wall roughness. If geometric similarity is to be maintained, the absolute magnitude of wall roughness must decrease as element size decreases. This can be a serious restriction to the use of simplified scaling information when making miniature elements. In the spirit of our earlier discussion, there is another parameter to be considered, ϵ/L, where ϵ is a characteristic roughness size.

It is interesting to note that the effect of roughness and of Mach number can enter together, as qualitative tests on a miniature boundary layer separation device dramatically showed. The effect of a roughness element at Mach number near unity can be much more drastic than at low Mach number, especially if at the higher Mach number the roughness element size is a larger fraction of the channel size than it is at low Mach number. We made an element with

nozzle width of 1/16", geometrically similar to the "1/4" nozzle width element. To operate this small element at Re = 30,000, it was necessary to operate at M = 0.8 instead of M = 0.4 for the boundary layer element. High Reynolds number performance of the small element became essentially identical with that of the large element only after the small element was carefully hand sanded, presumably so that it became relatively as smooth as the larger element. To date we have not separated the effects of roughness with and without Mach number changes.

(e) Instability

As reported by Orner, the free jet exhibits large oscillations when the outlet pressure becomes sufficiently high. This instability is an important limitation in the use of the element. The investigation of this instability is the subject of separate research, and is beyond the scope of the present scaling investigation.

VORTEX ELEMENT

(1) General Description

This is an element in which a basic radial inflow (supply) is controlled by a tangentially entering control flow. The resulting flow pattern can be idealized as having spiral streamlines; the presence of side walls means that there must also be axial flow. If the outlet pressure is held fixrd, then the radial component of velocity requires that the local pressure be higher than outlet pressure within the vortex chamber. This higher pressure can decrease, or even stop, a supply flow coming from a fixed pressure supply reservoir. Again this type of element is well known. The detailed geometry is shown in Figure 11. It is the one investigated by P. E. Koerper (Ref 3). We characterize the performance by the same parameters already discussed for the bistable and proportional elements, but without a vent.

(2) Performance Parameters

The basic variables are:

$$p_{s_t},\ p_{c_t},\ p_o,\ Q_s,\ Q_c,\ Q_o,\ \rho,\ \mu,\ a,\ L_1,\ L_2, \tag{10}$$

again we eliminate one flow rate through conservation of mass, and now measure pressure differences from outlet pressure. Hence the pertinent set of variables is:

$$(p_{s_t} - p_o),\ (p_{c_t} - p_o),\ Q_s,\ Q_c,\ \rho,\ \mu,\ a,\ L_1,\ L_2 \tag{10}$$

This is a set of 9 variables; we now form six independent non-dimensional parameters:

$$\frac{p_{c_t} - p_o}{p_{s_t} - p_o},\ \frac{Q_c}{Q_s},\ \frac{L_2}{L_1},\ \frac{\rho Q_o}{\mu L_2},\ \frac{(p_{s_t} - p_o)\ L_1^2}{\rho\ (Q_s/L_2)^2},\ \frac{Q_s}{L_1 L_2 a}, \tag{11}$$

Note the Reynolds number here is based on a representative average radial velocity and a corresponding representative circumference; that is:

$$Re = \frac{\rho V_{avg}\ (2\pi r)}{\mu} = \frac{\rho Q_o}{\mu L_2 (2\pi r)}\ (2\pi r) = \frac{\rho Q_o}{\mu L_2}$$

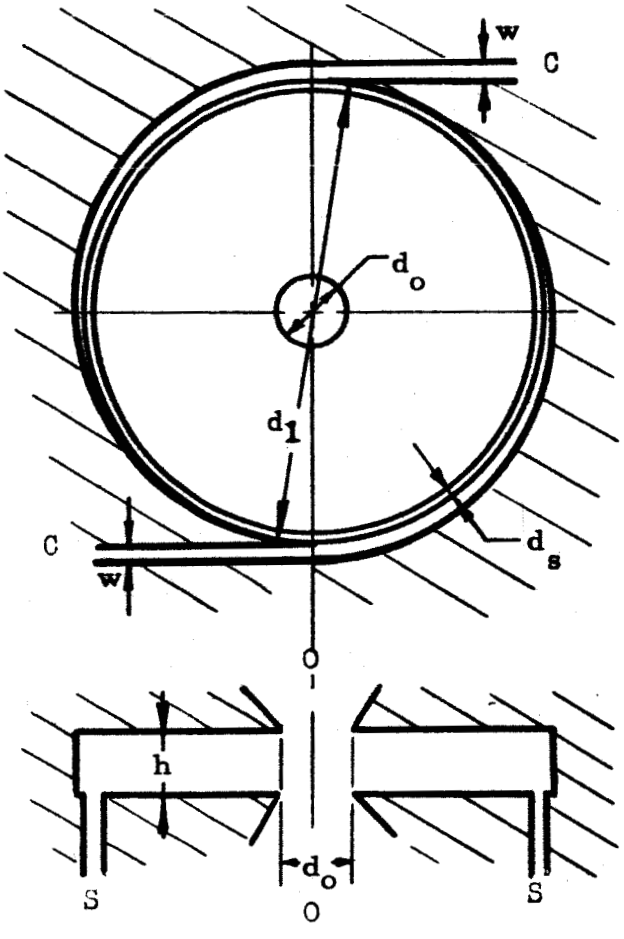

Where; $L_1 = w$ $L_2 = h$

$$\bar{D} = \frac{d_o}{d_1}, \quad \bar{D}_s = \frac{d_s}{d_1}, \quad \bar{H} = \frac{h}{d_1}, \quad \bar{W} = \frac{w}{d_1}$$

Figure 11 VORTEX AMPLIFIER

Repeating the previous arguments leads to a reduced set of parameters; we can write the reduced set as a functional equation analogous to equations (4) and (9):

$$\frac{Q_c}{Q_o} = f\left[\frac{p_{c_t} - p_o}{p_{s_t} - p_o} \;,\; \frac{\rho Q_o}{\mu L_2} \;,\; \frac{L_2}{L_1}\right] \qquad (12)$$

Note that $\frac{Q_o}{Q_s} = \left[1 - \frac{Q_c}{Q_o}\right]^{-1}$ for this element. For plotting the data, it is a little more convenient to use Q_c/Q_o here, rather than Q_o/Q_s, which was used for the other elements.

In the spirit of the scaling study, we should discuss the investigation of geometrically similar devices. However, a reasonable amount of work was done on the effects of geometrical variations. Since this work brought out important special features, and since the performance can be expressed in a reduced fashion with geometrical variation, some of the work including geometrical variation is also presented. For scaling purposes we will refer to an optimized element. The optimum element is designed for a maximum ratio of $\frac{Q_{o_{max}}}{Q_{o_{min}}}$ (Ref 4.)

(3) Experimental Procedure

Measurements were made on variable geometry elements, and on elements with removable inserts for geometrical variations. Measurements were made in the manner previously discussed for the bistable element. In this element, note that the outlet was at pressure of the room, and that there is no other vent.

(4) Experimental Results

(a) Flow Rate Pressure Ratio Curves

These curves are shown in Figure 12, for a Reynolds number range of 9,700 to 91,000, for air operation. Curves are drawn for two different geometries.

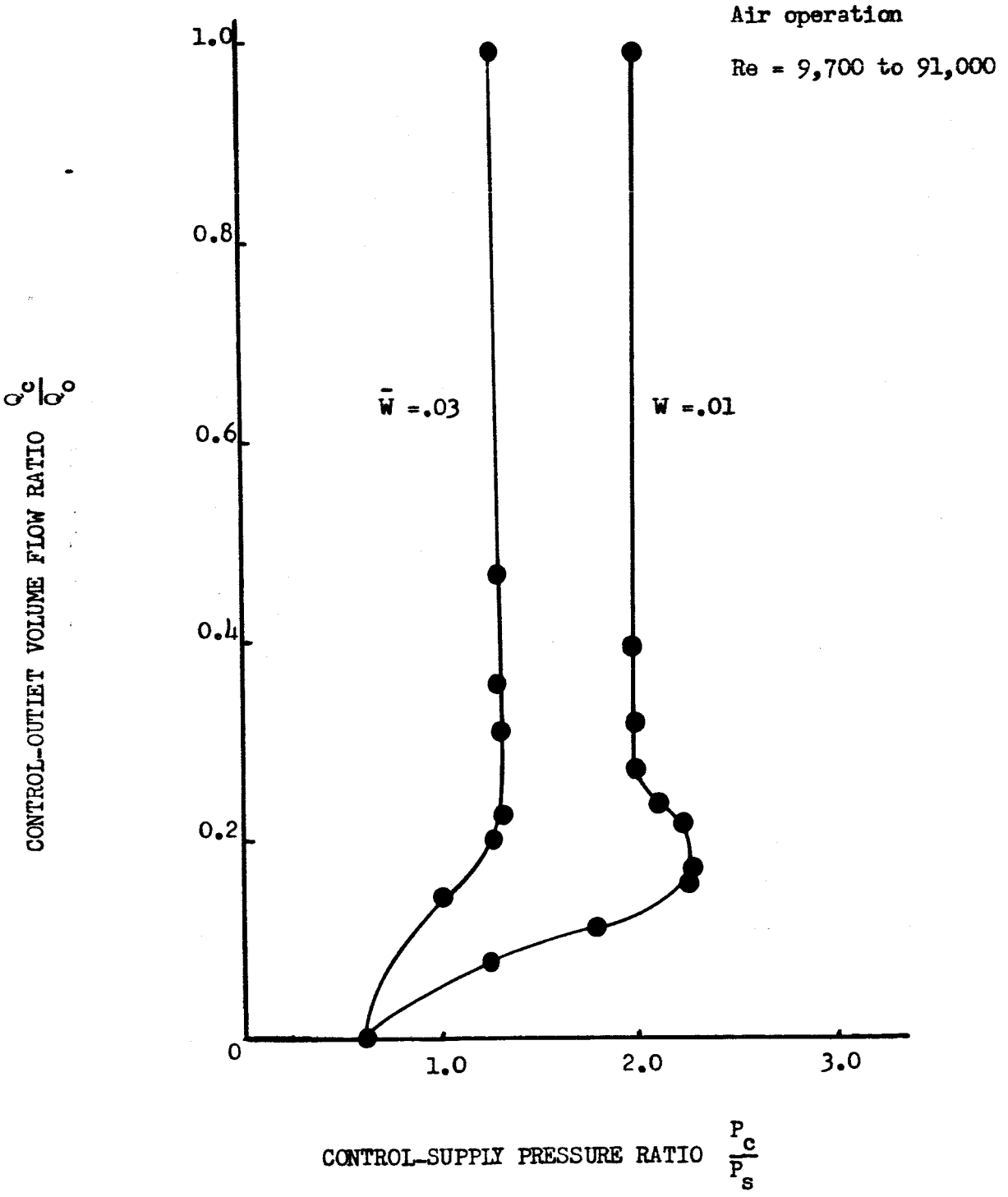

FIGURE 12 FLOW-RATE PRESSURE RATIO CURVES

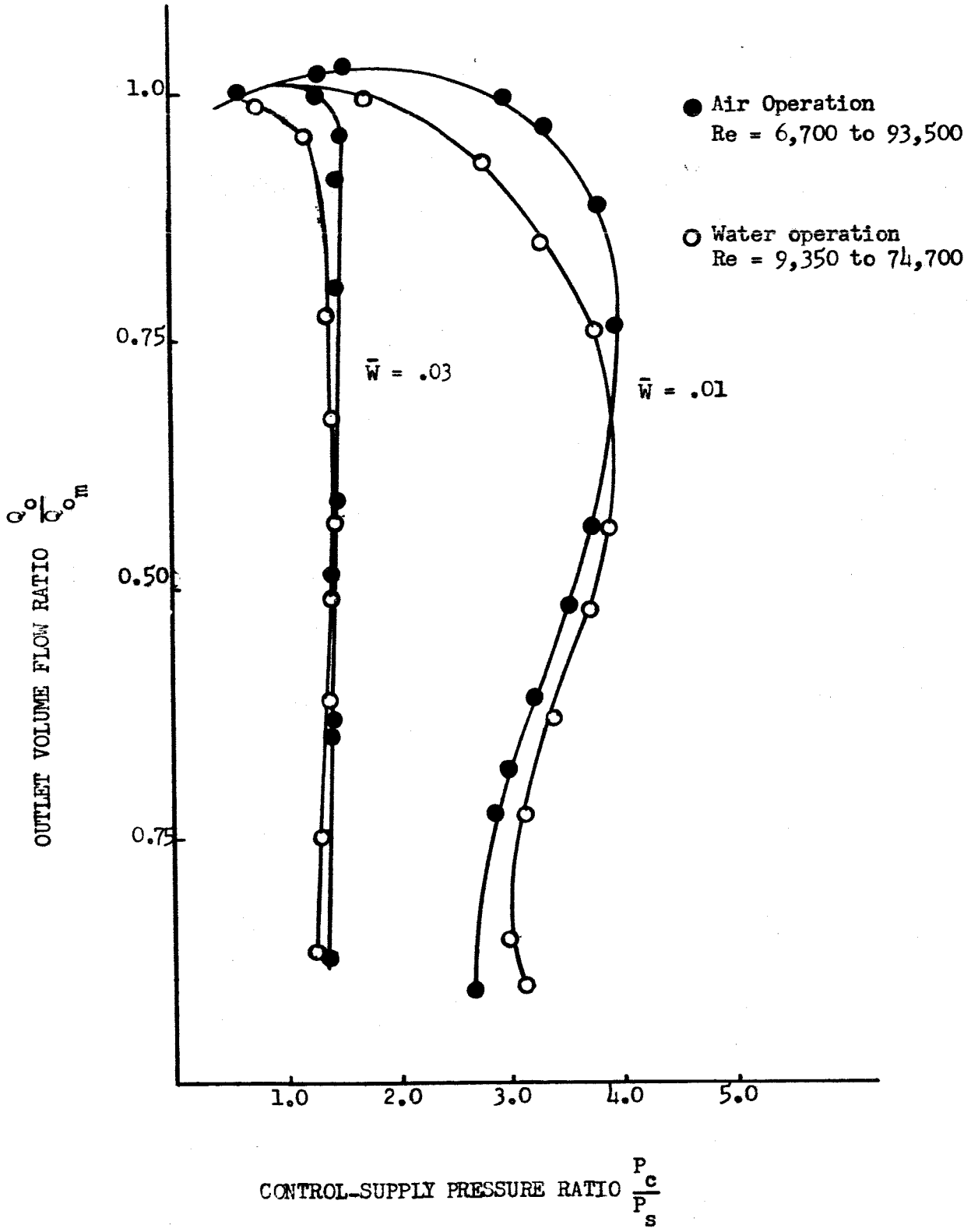

FIGURE 12a FLOW-RATE-PRESSURE RATIO CURVES

Note that the large range of Reynolds number is a little deceptive, because it is obtained primarily by varying control flow rate. A more searching test of the role of Reynolds number appears in the diode limit operation, to the discussed in section (d) below.

Corresponding curves for both air and water operation are shown in Figure (12a). In Figure (12a) the outlet flow rate is non-dimensionalized with respect to Q_{o_m}, where Q_{o_m} is the outlet flow rate with zero control flow; at this condition, $Q_o = Q_s$. The different non-dimensionalization is used because these tests were made without separately monitoring supply or control flow. They are presented so that air ans water operation can be shown together, and for completeness.

(c) Hysteresis

It is observed that under some conditions the flow rate-pressure ratio curves exhibit hysteresis. In the high Reynolds number limit, the hysteresis is associated with variations of planform, it not present in the optimized element, and does not have direct bearing on scaling. A scaled hysteretic element should maintain its hysteretic behavior, and a scaled non-hysteretic element should continue to be non-hysteretis. Examples of hysteretic behavior are shown in Figure 13. Hysteresis can be avoided by making the outlet and control flow holes sufficiently large.

Air Operation

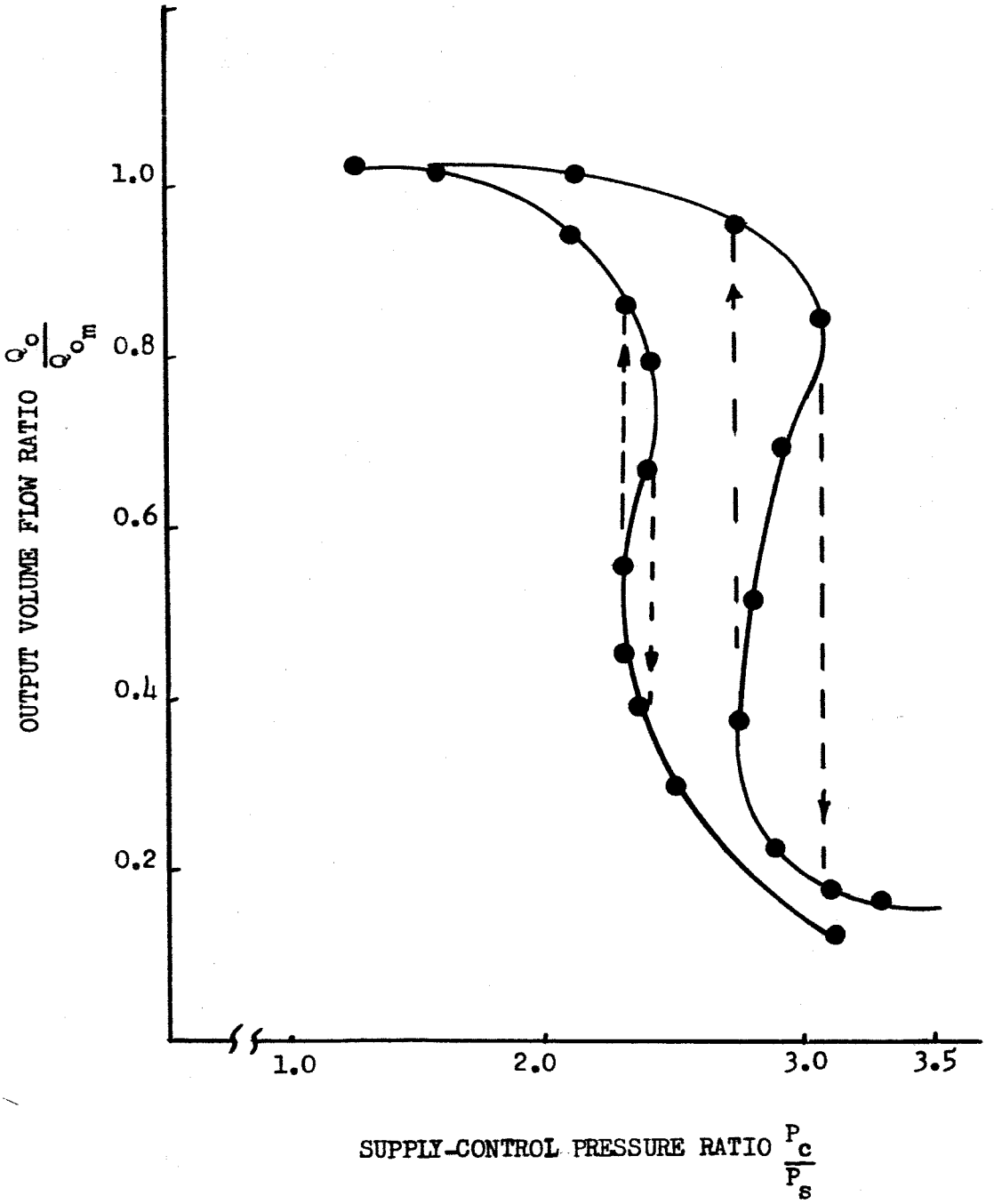

FIGURE 13 TYPICAL FLOW-PRESSURE CURVES WITH HYSTERESIS

(d) Grouping of Parameters

Reduction of parameters by grouping of parameters, and also the high Reynolds number limit, is strikingly shown for the performance of this element with geometrical variations and with no supply flow, in what is called the diode limit. For this element there is a simple two-dimensional non-viscous limit in which the flow is regarded as the superposition of a vortex flow and a sink flow. This result is

$$\frac{p_{s_t} - p_o}{\frac{1}{2}\rho\left(\frac{Q_o}{2wh}\right)^2\left[\left(\frac{d_1}{d_2}\right)^2 - 1\right]} \approx 1 \qquad (13)$$

or $$\overline{\Delta P} \approx 1 \qquad (14)$$

The left hand side can be regarded as a stretched pressure coefficient. With viscous effects, one expects:

$$\overline{\Delta P} = f\left(\frac{Q_o}{\nu h}, \frac{w}{d_1}, \frac{d_1}{d_o}\right) \qquad (15)$$

The data plotted according to equation (15) is shown in Figure 14. Qualitative reasoning suggests, however, that the variables in Equation (15) should group as follows:

$$\overline{\Delta P} = f\left(\frac{Q_o}{\nu h}, \frac{w}{d_1}, \left(\frac{d_1}{d_o}\right)^{1/2}\right) \qquad (16)$$

That is, the three variables become one. The data plotted according to equation (16) is shown in Figure 15. Both Figures 14 and 15 show that the non-viscous result, $\bar{P} = 1$, is approached as the Reynolds number goes to infinity. Figure 15 show the compacting of the several curves of Figure 14 into one curve, an important scaling simplification.

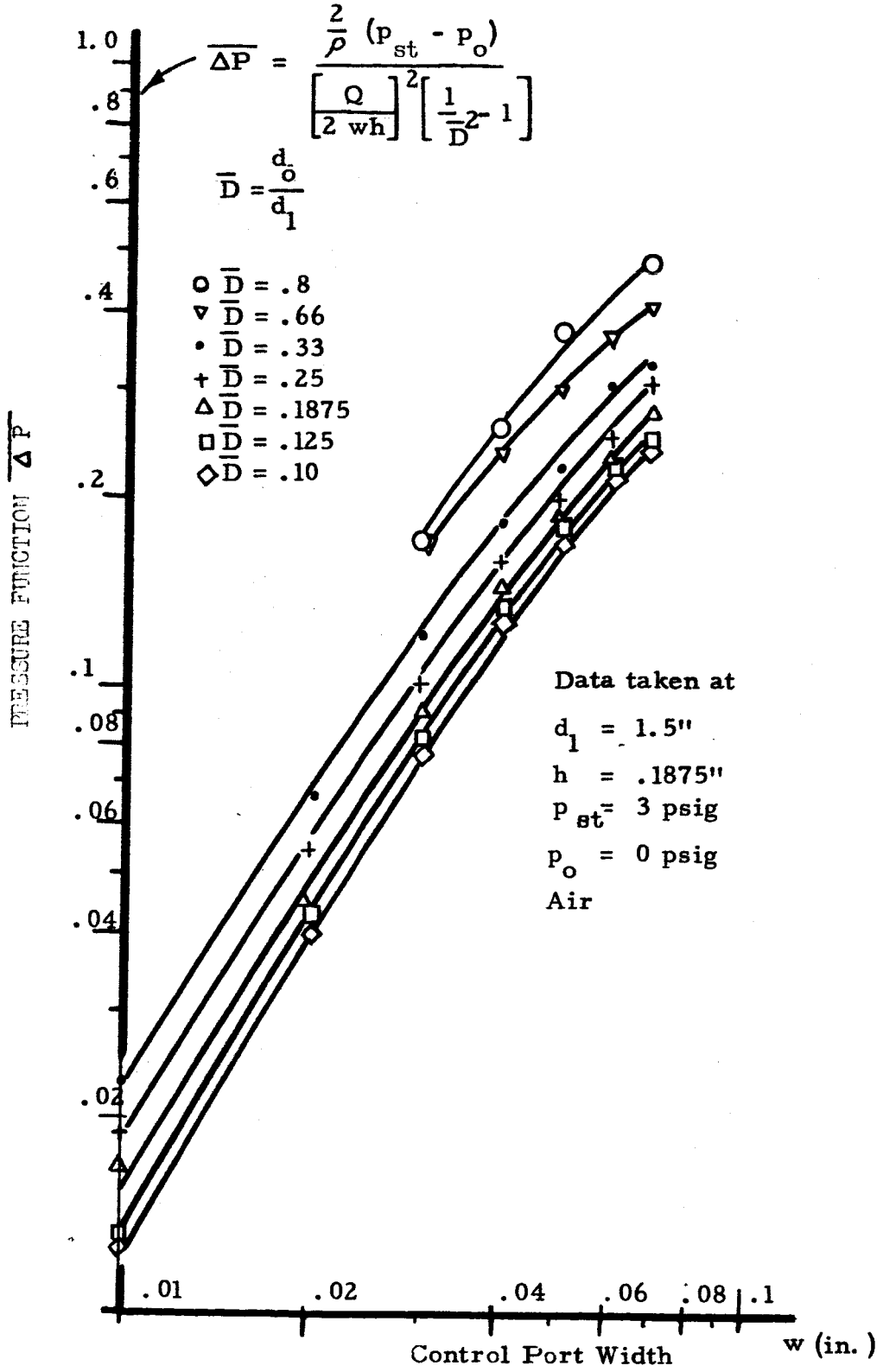

Figure 14 PRESSURE FUNCTION VARIATION IN DIODE OPERATION

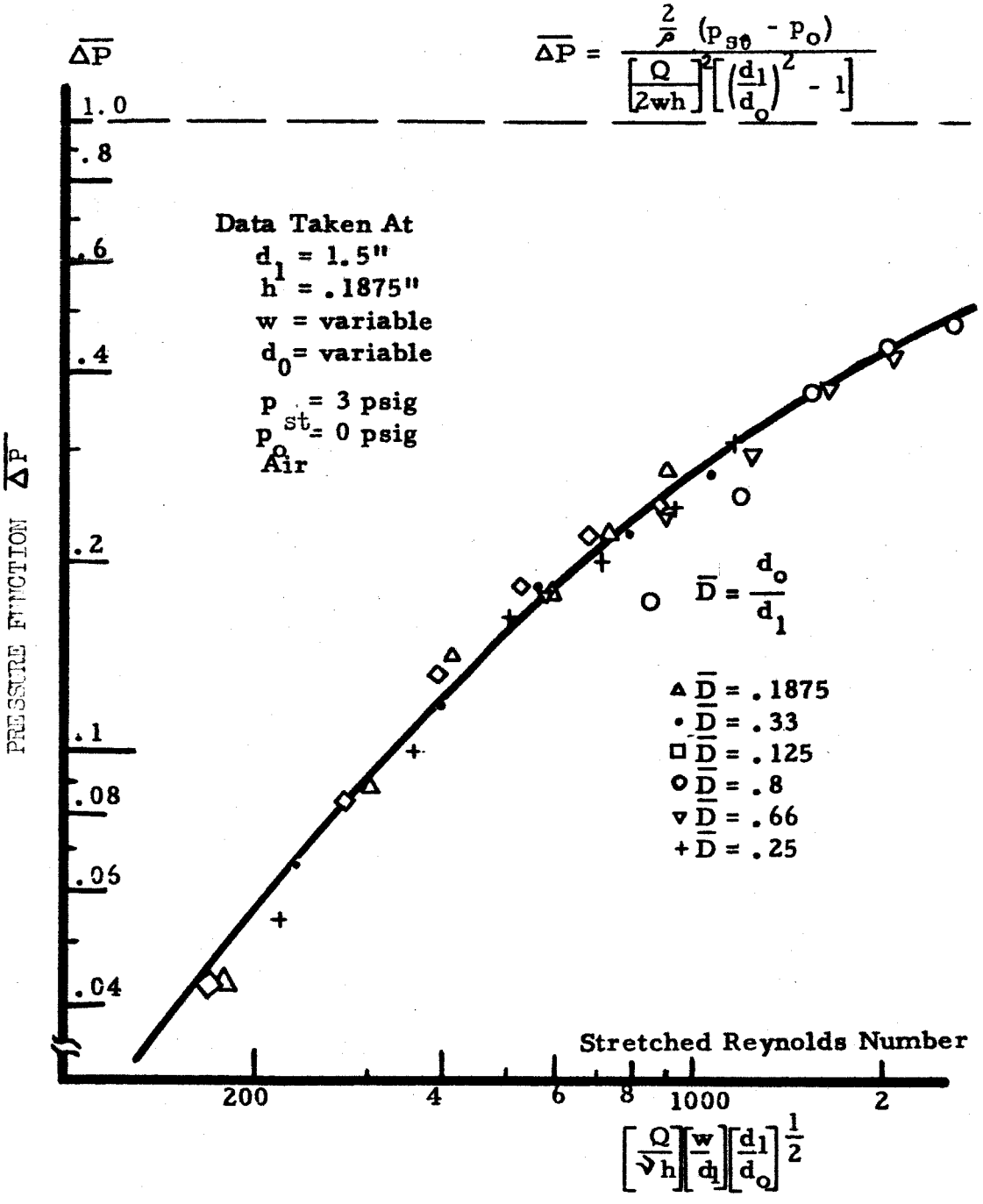

Figure 15 PRESSURE FUNCTION VARIATION WITH STRETCHED REYNOLDS NUMBER IN DIODE OPERATION

(e) Suggested grouping of Parameters with Supply Flow

Going to operation with supply flow, one expects that the performance will be expressible in the same manner as Equation (16) with $\frac{w}{\pi d_1}$ replaced by $\frac{V_r}{V_t}$.

$$\text{But } \frac{V_r}{Vt} = \left[\frac{A_c}{A_s} \quad \frac{Q_s}{Q_c} + \frac{w}{\pi d_1}\right] \quad f\left({}^{Q_c}/_{Q_s}\right) \tag{17}$$

${}^{v_r}/_{v_t}$ should approach ${}^{\omega}/_{\pi d_1}$ as ${}^{Q_c}/_{Q_s}$ approaches infinity, and should approach infinity as ${}^{Q_c}/_{Q_s}$ approaches zero. This means that $f({}^{Q_c}/_{Q_s})$ should approach 1 as ${}^{Q_c}/_{Q_s}$ approaches infinity, and should be non-zero (or at least not go to zero as fast as ${}^{Q_c}/_{Q_s}$) as ${}^{Q_c}/_{Q_s}$ approaches zero. Note that $f({}^{Q_c}/_{Q_s} = 1$ meets both these requirements. Unfortunately our data is not sufficient to test this compacting, which should therefore be regarded as a suggestion.

In terms of geometrically similar scaling, the suggested compacting can be viewed as follows: Equation (12) can be reinterpreted as

$$\frac{Q_c}{Q_s} = f\left[\frac{p_{c_t} - p_o}{p_{s_t} - p_o}, \quad \frac{\rho Q_o}{\mu L_2}; \quad \frac{L_2}{L_1}\right] \tag{18}$$

The compacting is equivalent to writing:

$$\left({}^{Q_c}/_{Q_s}\right) \; F_1 = f\left[\frac{\rho Q_o}{\mu L_2} \quad F_2; \quad \frac{L_2}{L_1}\right] \tag{19}$$

In the geometrically similar elements, the compacting serves to reduce the number of variable by one.

Since power $\propto (\Delta p)UL^2$, and since c_p is now fixed, this means power $\propto 1/L$. So the choice of a desirable Reynolds number means that power consumption increases with decreasing element size. Note that the pressure difference $(1/L)^2$, and the mass flow rate $\propto L$.

In order to keep perspective, we look for a moment at response time, despite the fact that the study herein is for steady flow. The response time is characterized by the ratio $\frac{t_{response}}{t_{flow}} = \frac{u}{\omega L}$. With the restrictions mentioned, $\frac{u}{\omega L} = f\ (Re\ ;\ M)$. If a choice of a desireable Reynolds number is made, then we see that $\omega \propto 1/L^2$. It should be kept in mind, however, that the desireable Re . no. might be different for fast response than it is for low power. Furthermore, the parametric respresentative is too simple as given above, but a deeper discussion of unsteady effects is beyond the scope of this study. At this point it suffices to say that, with an optimum Reynolds number chosen (and this can generally be done), size reduction yields faster, but more power consuming elements, requiring larger pressure differences but handling smaller mass flows. Similar qualitative statements can be made about other quantities of interest, reasoning from the scaling laws presented.

Work to be Done

Purely with regard to scaling, the following extensions of this study would be useful:

(1) Effects of compressibility (Mach number scaling).

(2) Performance scaling of individual elements in non-steady operation.

(3) Performance scaling of interconnected elements in steady operation.

(4) Performance scaling of interconnected elements in non-steady operation.

(5) Choices of desireable parameters, and scaling laws with these choices.

(6) Scaling laws for optimized circuits.

Qualitative Discussion of Size Changes

The foregoing has discussed how the performance of these elements can be expressed in terms of a small number of non-dimensional parameters. These give the scaling laws in a simpler form than is indicated by a complete dimensional analysis. The manner of analysis suggests that the reduction of parameters should hold for other elements than the ones investigated herein.

It is useful now to consider the designer's question "so what does happen when I change element size?" To clarify this question, it is convenient to consider a single fluid, a fixed aspect ratio, and fixed pressure difference ratios (this still allows a pressure coefficient to vary).

Let us think in terms of the bistable device, recognizing that our statements are actually more general. With the restriction just mentioned, we rewrite equation (4a):

$$\frac{(p_{s_t} - p_v)\, L_1^2\, L_2^2}{\rho\, Q_s^2} = f\left(\frac{\rho\, Re}{L_2}\right)$$

or, for simplicity and generality,

$$c_p = f\ (Re\ ;\ M)$$

The choice of a desirable Reynolds number is not clear. If the criterion is ease of circuit design, then one wants to operate at a Reynolds number suffiently high so that the performance is Reynolds number independent. If one wants to keep power consumed to a minimum, then one wants to operate at the minimum possible Reynolds number; this is true even recognizing that characteristic skin friction coefficients decrease with increasing Reynolds number, for either laminar or turbulent flow (but not, of course, if one goes from laminar to turbulent flow). For Reynolds number independence and low power consumption, one chooses as low a "sufficiently high" Reynolds number as possible. Having chosen a desirable Reynolds number, then the product UL is fixed (again, with the previous restrictions).

List of References

1. Wilson, J. N. "A Fluid Analog to Digital Conversion System", Engineering Design Center Report EDC 7-64-4, Case Institute of Technology, September, 1964.

2. Orner, P.A. "A Fluid Amplifier Controlled Pneumatic Turbine Servomechanism", Engineering Design Center Report EDC 7-64-5, Case Institute of Technology, October, 1964.

3. Koerper, P. E. "Design of an Optimized Vortex Amplifier", Engineering Design Center Report EDC 7-65-6, Case Institute of Technology, 1965.